ELSEVIER

Journal of Molecular Catalysis B: Enzymatic 16 (2002) 241–247

JOURNAL OF MOLECULAR CATALYSIS B: ENZYMATIC

www.elsevier.com/locate/molcatb

Lipase-catalyzed regioselective acylation of resorcin[4]arenes

Bruno Botta [a], Giovanni Zappia [a], Andrea Tafi [b,*], Maurizio Botta [b], Fabrizio Manetti [b], Enrico Cernia [c], Giuliana Milana [c], Cleofe Palocci [c], Simonetta Soro [c], Giuliano Delle Monache [d]

[a] *Dipartimento di Studi di Chimica e Tecnologia delle Sostanze Biologicamente Attive, Università La Sapienza, P. le A. Moro 5, I-00185 Rome, Italy*

[b] *Dipartimento Farmaco Chimico Tecnologico, Università degli Studi di Siena, Via A. Moro snc, I-53100 Siena, Italy*

[c] *Dipartimento di Chimica (NEC), Università La Sapienza, P. le A. Moro 5, I-00185 Rome, Italy*

[d] *Centro Chimica dei Recettori, Università Cattolica del S. Cuore, Largo F. Vito 1, I-00168 Rome, Italy*

Received 14 June 2001; accepted 4 October 2001

Abstract

Immobilized lipase from *Mucor miehei* (RML) catalyzed the regioselective acylation of the C-2 side-chain of the C-alkyl resorcin[4]arene tetra-alcohol **1** in the 1,2-alternate form in organic solvents using vinyl acetate as acylating reagent. The influence of reaction parameters and solvent choice were also studied. Docking simulations allowed the determination of the binding geometry of **1**, revealing the importance of Trp88 residue in stabilizing the Michaelis–Menten complex between enzyme and substrate. © 2002 Elsevier Science B.V. All rights reserved.

Keywords: Resorcinarene; Lipase; Transesterification; Molecular modeling; Docking

1. Introduction

Microbial lipases of various sources have found numerous applications in organic synthesis, because they combine a broad substrate-specificity with a high stereoselectivity and regioselectivity. They are easily accessible and do not require expensive and unstable coenzyme systems.

For several lipases, crystallographic data are available [1,2], which provide their three-dimensional structures, while sophisticated molecular modeling softwares allow to study the interactions among a substrate and the amino acids of the catalytic site.

In most cases, the proposed enzyme–substrates interaction models for lipase selectivity, however, can be used to predict reactivity only for substrates similar to those already tested [3–5].

In this work, we first deal with the chemical studies and computer calculations on lipase-catalyzed transesterification reactions of resorc[4]arenes in different organic solvents.

Lipase-catalyzed transesterifications have been used to produce inherently chiral calix[4]arene derivatives with an enantiomeric excess (ee) of upto 100% [6]. Conversely, we chose as a substrate the synthetic C-alkyl-resorcin[4]arene **1** [7] with a 1,2-alternate configuration, characterized by a C_s symmetry and the presence of a unique symmetry plane passing through C-2 and C-14 carbons. The side-chains at C-8 and C-20 are equivalent and in a *cis* arrangement with

* Corresponding author. Tel.: +39-0577-234313; fax: +39-577-234333.
E-mail address: tafi@unisi.it (A. Tafi).

1381-1177/02/$ – see front matter
PII: S1381-1177(01)00068-6

respect to the C-2 substituent, but with the C-14 alkyl chain located in a *trans* position, they are potential sources of desimmetrization. Owing to the presence of different regioisomeric hydroxyl functions, two prochiral centers, and a challenging large size, the calixarene **1** appeared to be an intriguing substrate in order to obtain further information for the development of a rational model of enzyme–substrate interactions.

2. Experimental

2.1. Reaction conditions

Immobilized lipase from *Mucor miehei* (RML) was purchased from Novo Nordisk (Denmark). All solvents were supplied by Aldrich. Acetonitrile and water were HPLC grade.

The preparation of resorcin[4]arene tetraalcohol **1** has been previously reported [7]. The fully acetylated compound **3** was obtained by a standard procedure (with pyridine/acetic anhydride).

Acylation reactions were carried out in 1 ml of organic solvent containing compound **1** (0.013 M), vinyl acetate as acyl donor (1.08 M) and immobilized RML (75 mg). The mixture was incubated at 40 °C for 48 h under magnetic stirring at 600 rpm. Progress of the reaction was followed by periodical analysis of 50 μl aliquots of the reaction mixture dissolved in 1 ml of acetonitrile by HPLC (Perkin-Elmer) on a C-18 reversed-phase column using acetonitrile/H_2O 60/40 as eluent. UV detector (Jasco-UV 975) was used at 283 nm. Hydrolysis reactions with partially acetylated compounds **2** and **4** were performed in phosphate buffer (10 mM, pH 7.5) and a biphasic system (buffer:chloroform 2:1) under the same acylation conditions. Blank experiments (without enzyme) were also run.

2.2. Molecular modeling

Calculations and graphic manipulations were performed on a Silicon Graphics workstation Indigo R4000. The software package MacroModel/Batchmin (version 4.0) [8], equipped with the Amber* united atoms force field, was used in this study to perform all the calculations. Solvent effects were not taken into account.

The Cartesian atomic co-ordinates of the enzyme utilized for the docking experiments were obtained from the X-ray structure of RML in the pdb file (structure code 4TGL) [9] available from the Brookhaven Protein Data Bank, and were used without further refinement by energy minimization. Hydrogen atoms were added only to the heteroatoms of the model, whereas crystallization water molecules were not included in the calculations.

The Batchmin Monte Carlo multiple minimum methodology (MCMM) was chosen to carry out a flexible docking simulation, which consisted in random rototranslations of **1** coupled with a statistical conformational search, inside the active site. Because of the high number of translational, rotational and conformational degrees of freedom, our computational power did not allow a single exhaustive run. Therefore, several consecutive runs (each one made of 5000 Monte Carlo steps) with different starting geometries of **1** and different sequences of random numbers were performed.

For each Monte Carlo step the rototranslations of **1** (around the C-2 atom) were limited by the maximum values of 180° for the rotational angle and of 15 Å for the translational movement. At the same time the 12 rotatable bonds of the side-chains of both **1** and the residues 144 and 88 were subjected to random step variations of the torsion angles in the range 60–l80°.

The crystallographic structure of the enzyme was fixed in three-dimensional space during the runs. To speed up the calculations, instead of the large number of atoms of the whole system (2575), an internal region of acetyl-RML, centered on Ser 144 and comprising all the aminoacids with at least one atom within a distance of 12.0 Å was considered for the minimization [10]. The intramolecular distances among the residues of the catalytic triad were monitored during the experiments as to maintain relative orientations compatible with the mechanism of the hydrolysis reaction.

The **1**-acetyl-RML complexes found in the MCMM procedure were subjected to energy minimization until a derivative convergence of 0.01 kJ/Å mol was reached. A set of 20 atoms, 12 in the substrate and 8 in the enzyme, were selected in order to compare each new minimized output structure with all the previous minima. All the complexes, whose minimum energy was more than 50.0 kJ/mol over those previously found, were rejected.

Two further constraints were imposed in performing energy minimization of the complexes: (a) in addition to the catalytic triad, the side-chains of six residues inside the subset and located on the walls of the active site (namely: Trp88, Val205, Leu208, Val254, Leu258 and Leu267) were fully minimized together with the substrate to guarantee the complementarity between the surfaces of the two partners; (b) all the other atoms of the internal subset were fixed in three-dimensional space, even though their non-bonding interactions with all the relaxing atoms were calculated.

3. Results and discussion

3.1. Structure of products and analytical studies

The RML-catalyzed reaction of substrate **1** with vinyl acetate at 40 °C in different organic solvents, chosen according to the solubility of **1**, afforded mainly the product **2**. The highest percentage of conversion after 48 h (Table 1) was obtained for **2** in chloroform (90% yield), whereas it remained around 80% for most of the other solvents. Only when benzene was used as a solvent, a minor diacetylated product **4** (15% yield) was also obtained. No reaction took place in blank experiments.

In order to investigate the enzyme regioselectivity for *the* C-2 position, the monoacetylated resorcin[4]arene **2** was used as a substrate for successive transesterifications in the same solvents. The conversion to the diacetylated derivative **4** did not exceed 10%, with the predictable exception of benzene (24% yield). On the other hand, in order to test the reaction reversibility, attempts to hydrolyze the acetyl derivatives **2** and **4** in aqueous or biphasic systems were performed, but no hydrolysis product was obtained.

Since the lipase activity in a medium has been often correlated with its physico-chemical properties, we took into consideration $\log P_{ow}$ and dielectric constant ε of the selected solvents (Table 1).

Hydrophobic solvents (high $\log P_{ow}$ values) are expected to stabilize the enzyme in the active conformation, not interacting with the essential water-layer around the protein [11]. Although the rates and the yields of the reaction seemed somehow to increase with the solvent hydrophobicity (Table 1), no significant fit was found by plotting. The electrostatic forces, that contribute to the stability of the tertiary structure of the enzyme in its active form, are also depending on the solvent dielectric constant [12]. However, no correlation was found between ε and the reaction rate (Table 1); e.g. comparable values of initial reaction rates were obtained for dioxane and acetonitrile, which have largely different dielectric constants.

In conclusion, the physico-chemical characteristics of the solvent seem to play a minimum role in the reaction, probably because of the large size of the substrate. The ^{1}H and ^{13}C NMR spectral data of the starting compound **1** are reported in Table 2 together with those of its acetyl derivatives. In the ^{1}H and ^{13}C NMR spectra of **1,** the signals of the bridge methine group, as well as those of the substituents, show a 1:2:1 distribution pattern. Notably, the proton signals of the C-14 alkyl chain are shifted highfield by the neighbouring aromatic rings [7]. On the other hand, carbons and protons of the aromatic rings (methoxyl groups included) are equivalent two by two and lead to half the number of signals (Table 2). The acetylation

Table 1
Conversion and initial rate of substrate **1** in different solvents[a]

Solvent	Conversion (%)	Initial rate (μmol/min)	Hydrophobicity ($\log P_{ow}$)	ε (20 °C, 1 atm)
Chloroform	90	2.80	2.0	4.81
Isopropanol	86	1.82	–	18.3
Tetrahydrofuran	85	2.32	0.49	7.4
Acetonitrile	83	1.20	−0.33	37.5
Dioxane	80	2.00	−1.1	2.21
Dichloromethane	77	2.20	0.93	9.08
Benzene	75	2.32	2.0	2.28
Acetone	58	1.20	−0.23	20.7

[a] $T = 40$ °C; [***1***] = 0.013 M; [vinyl acetate] = 1.08 M; Vr = 1 ml.

Table 2
^{1}H and ^{13}C NMR spectral data of resorcin[4]arenes[a]

	Compound				
	1	**2**	**4**	**4**	**3**
Carbon (δ_C)					
C-2	27.5	28.1	28.1		28.3
CH_2	40.0	35.7	35.9		35.7
CH_2O	61.3	63.7	63.8		63.7
C-8, C-20	31.3	31.2	31.9	32.1	32.0
CH_2	37.8	37.8	37.7	33.5	33.3
CH_2O	61.2	61.2	61.4	64.2	63.8
C-14	27.0	26.9	26.9		27.8
CH_2	39.6	39.5	39.2		35.0
CH_2O	60.9	60.8	60.9		63.1
Proton (δ_H)					
H-2	5.27 t (8)	5.21 t (8)	5.25 t (8)		5.22 t (8)
CH_2	2.19 dt (8, 6)	2.30 q (7.5)	2.36 td (8,6)		2.35 q (7.5)
CH_2O	3.56 t (6)	3.99 t (7.5)	3.99 t (7.5)		3.98 t (7)
H-8, H-20	4.75 t (7.5)	4.74 t (7.5)	4.70 t (6)	4.67 dd (9, 5)	4.70 dd (8.5,6.5)
CH_2	2.18 ddt (13, 7.5, 6)	2.18 dq (14, 7)	Not assignable		2.21 m
	2.01 ddt (13, 7.5, 6)	2.04 m			2.10 m
CH_2O	3.49 t (6)	3.53 m	3.61 m	4.28 dt (10, 6)	4.18 ddd (10.5, 8, 6)
				4.00 dt (10, 6)	3.90 ddd (10.5, 6, 2)
H-14	4.88 t (8)	4.88 t (8)	4.88 t (8.5)		4.80 t (8)
CH_2	1.24 dt (8, 6)	1.22 q (6)	1.23 q (6)		1.35 m
CH_2O	2.98 t (6)	2.96 t (6)	2.98 t (6)		3.46 t (6)

[a] 300 (^{1}H) and 75 (^{13}C) MHz, TMS as internal standard. Proton signals showed the appropriate integrate intensity. Coupling constants are given sequentially in parentheses.

(full in derivative **3**) of the alcoholic functions causes the expected downfield shift of the CH_2O signals in both ^{1}H and ^{13}C NMR spectra, as well as the high-field shift of the carbon signal of the neighbouring methylene (compare **1** and **3** in Table 2). These considerations established that in product **2** only the C-2 side-chain had been acetylated.

In the ^{1}H and ^{13}C NMR spectra of compound **4** (Table 2) the number of signals was the same as the number of protons and carbons, revealing that the plane of symmetry going through C-2 and C-14 was lost. This finding requires that one of the acetyl groups is either on the C-8 or on the C-20 side-chain. Being clearly the second acetyl group on the C-2 side-chain (Table 2), the product **4** was assigned the structure of a racemic mixture ($\alpha_D = 0$) diacetylated at C-2; C-8 and C-2; C-20. The FAB-MS spectral data of chain **2** and **4**, compared with those of **1** and **3** in Table 3, confirm the presence of one and two acetyl groups, respectively.

As for other C-alkyl resorcin[4]arenes [6] the mass spectra are characterized by the loss of the alkyl substituents, i.e. CH_2CH_2OH (45 nm) for **1** and $CH_2CH_2OCOCH_3$ (87 nm) for **3**. Obviously, the

Table 3
FAB-MS spectral data of resorcin[4]arenes[a]

	Compound			
	3	**1**	**2**	**4**
MH^+	777 (13)	819 (26)	861 (26)	945 (19)
M^+	776 (19)	818 (39)	860 (35)	944 (24)
$M - 45^+$	731 (100)	777 (100)	815 (100)	–
$M - 60^+$	–	758 (28)	800 (29)	884 (15)
$M - 87^+$	–	731 (20)	773 (21)	857 (100)

[a] 45 (CH_2CH_2OH); 60 (CH_3COOH); 87 ($CH_2CH_2OCOCH_3$).

partially acetylated **2** and **4** show both the losses and the intensity of the M-$CH_2CH_2OCOCH_3^+$ ion increases on going from **2** to **4**.

The effect of the concentration of the acyl donor in chloroform on the lipase-catalyzed acetylation rate of **1** was studied as a result, the initial rate increased with the increase of the concentration, giving the optimum value for 1.08 M vinyl acetate.

The influence of different amounts of immobilized lipase was also monitored and the maximum value of reaction rate was obtained with 75 mg of RML. Finally, we found a maximum initial rate (2.8 ± 0.2 μmol/min) at a temperature of 40 °C, whereas minor values were measured at 30 and 50 °C (2.2 and 2.6 μmol/min, respectively).

3.2. Molecular modeling studies

To shed further light on the substrate specificity and the regioselectivity of RML, we studied the acylation reaction of **1** by computational simulation. As it was not obvious which side-chains on **1** could preferentially react in the RML-catalyzed reaction, the calixarene-lipase recognition process was reproduced by flexible docking experiments following a protocol already defined in previous studies with lipase enzymes [10,13]. This approach was easier than the study, usually applied in biocatalysis, of the transition states or their analogues [14], since one single simulation was sufficient to explore the orientations relative to the appropriate active-site residues of all the four potentially reacting groups [15], and to produce a molecular model of the substrate–enzyme interaction.

According to the catalytic mechanism reported in the literature for RML and other lipases [16], the side-chain of Ser144 was modified from CH_2-CH_2-OH to CH_2-CH_2-OCO-CH_3 (Ser*144 thereafter) in order to reproduce the acetyl-enzyme supposed to be the active species cleaved by the nucleophilic side-chain of **1** to give **2**. The lowest energy conformation of **1** in the gas phase, previously calculated [7], was used as the starting geometry for several consecutive runs in the active site of acetyl-RML. During the docking, the side-chains of residues Ser*144 and Trp88 were also rotated by random increments in the range 60–180°, because Ser*144 needs to be at a bond distance from the hydroxyl oxygens of **1** to allow the acetylation. On the other hand, the Trp88 residue is reported to play a relevant functional role in RML [13], because it stabilizes the enzymatic complex by the formation of favourable π-interactions with the aromatic nuclei of the substrate.

Our analysis was limited to consideration of the geometry of docking complexes and no attempt was made at this stage to correlate quantitatively their steric energies and enzyme activity, because, as previously discussed [17], the applied restraints might provide misleading values.

The **1**-acetyl-RML output complexes, collected from several runs, revealed two possible families (**A** and **B**) of low-energy recognition geometries of **1**. Family **A**, whose lowest energy structure was the global minimum (Fig. 1), showed three of the side-chains at C-2, C-8, and C-20 of the ligand molecule directed towards the enzyme binding site, whereas the fourth side-chain at C-14 extended in the outer direction. By contrast, in family **B**, as shown in Fig. 2 for the lowest energy complex with this geometry, the side-chain at C-14 was directed towards the active site catalytic Ser*144, whereas the other three side-chains were pointing outside. In both cases, the π-interactions of the residue Trp88 with the aromatic rings of **1** were favoured. In geometry **A**, the Trp88 aromatic system and the B phenyl ring of the ligand were almost parallel at a distance between the centroids of the two nuclei of 3.6 Å. Conversely, in geometry **B**, the centroid of the Trp88 aromatic system was approximately located in front of C-8 atom of **1**, forming an angle of ca. 30° with the planes of both the C phenyl ring (at distance of 4.0 Å) and the D phenyl ring (at distance of 3.8 Å), respectively. However, the calixarene nucleus is so severely distorted in geometry **B** that the full C_s symmetry of the 1,2-alternate conformation is lost indeed, the C and D phenyl rings had to be rotated to give the already described favourable interactions with the Trp88; as a result, the conformation of the macrocycle oscillates between those of 1,2-alternate and the flattened partial cone. On the contrary, the C_s symmetry of **1** was maintained in geometry **A**.

The global minimum (Fig. 1) shows that the side-chain of C-2 in **1** is correctly oriented towards the residues of catalytic triad (Ser*144, His 257 and Asp 203) [9], so that it may undergo the acylation reaction. In particular, the hydroxyl group of the side-chain of

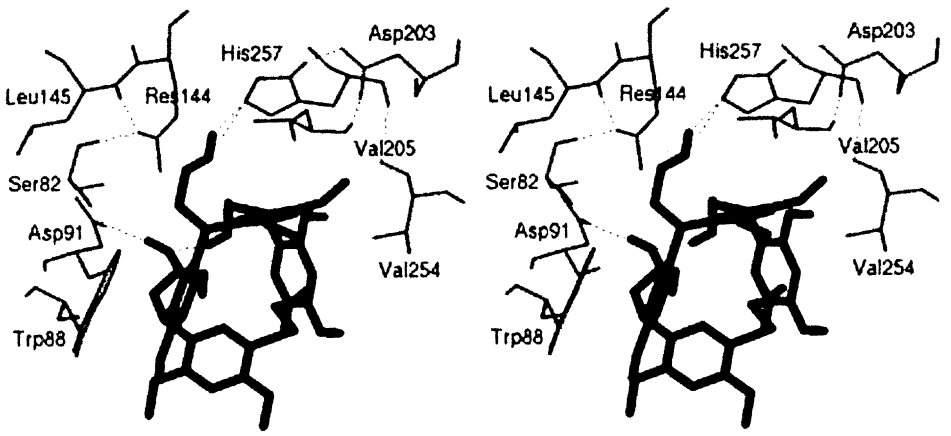

Fig. 1. Stereo view of the calculated recognition geometry **A** of **1** (thick line) in acetyl-RML. For the sake of simplicity only the lipase residues useful for the discussion are shown. Hydrogen atoms bound to heteroatoms are displayed. Hydrogen-bonding interactions are depicted as dotted lines.

1 is located in the region of three-dimensional space comprised between Ser*144 and His257 and acts as hydrogen-bond donor to the imidazole ring of His 257, which, in turn, is hydrogen bonded to Asp 203. Moreover, in the oxyanion hole, the carbonyl oxygen of Ser*144 and the backbone NH of the residues Ser82 and Leul45 already form the hydrogen bonding interactions that are postulated to stabilize the tetrahedral intermediate [10,13]. The π-stacking interaction between **1** and the aromatic ring of Trp88 is also clearly shown in Fig. 1. Finally, the C-20 side-chain of the ligand interacts by hydrogen bonding with the side-chain of Asp 91 and the side-chain of C-8 of **1** (Fig. 1). In conclusion, all the above findings are in agreement with the catalytic mechanism proposed for RML [9] and with the experimental results.

In the case of geometry **B** (Fig. 2), on the contrary, the hydroxyl group of the side-chain at C-14 would act as hydrogen donor to the Asp9l residue and the other

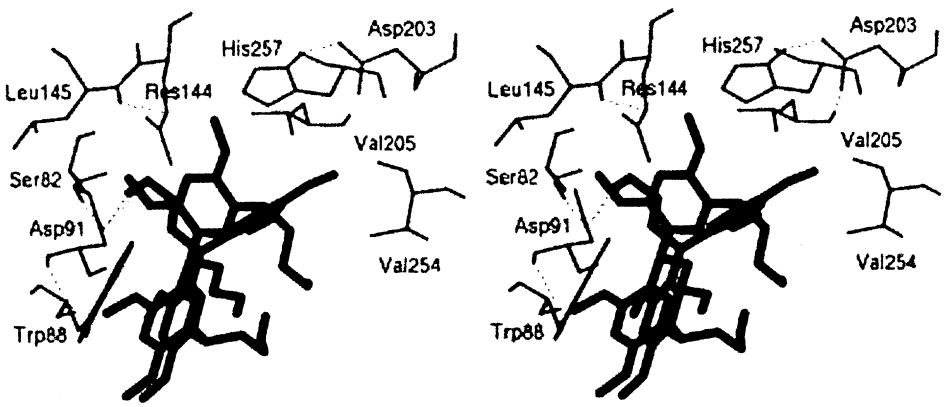

Fig. 2. Stereo view of the discarded output docking geometry of **1** (thick line) in acetyl-RML (geometry **B** in the text). For the sake of simplicity only the lipase residues useful for the discussion are shown. Hydrogen atoms bound to heteroatoms are displayed. Hydrogen-bonding interactions are depicted as dotted lines.

three side-chains of the ligand would point outside, while one of the two methoxy groups of ring B would be located in the region of three-dimensional space comprised between the catalytic residues 144 and 257.

4. Conclusions

Immobilized lipase from *Mucor miehei* was shown to catalyze the regioselective acylation by vinyl acetate of the C-2 side-chain of the C-alkyl resorcin[4]arene tetra-alcohol **1** in the 1,2-alternate form. The enzyme partially acetylated the prochiral side-chains at C-8 and C-20, but did not produce desimmetrization. The choice of the solvent influences the yield of the trans-esterification reaction, and poorly, the regioselectivity of the acylation. Attempts to correlate the enzyme activity with the physico-chemical properties of the organic solvent revealed only a partial dependence upon the hydrophobicity of the medium.

Docking studies were extremely useful to rationalize the experimental results and allowed the identification of a molecular model for the substrate–enzyme interaction: they confirmed, in fact, the different availability of the C-2 and C-14 side-chains and revealed the importance of Trp88 residue in stabilizing the complex between enzyme and substrate.

Acknowledgements

The authors gratefully acknowledge the financial support of Programma Biotecnologie MURST-CNR (legge 95/95), Ministero Università, Ricerca Scientifica e Tecnologica (MURST) and CNR Target Project on Biotechnology.

References

[1] M.M.G.M. Thunnissen, E. Ab, K.H. Kalk, J. Drenth, B.W. Diijkstra, O.P. Kuipers, R. Dijkman, G.H. De Haas, H.M. Verhey, Nature, London 347 (1990) 689 and references therein.
[2] M. Nardini, D.A. Lang, K. Liebeton, K.-E. Jaeger, B.W. Dijkstra, J. Biol. Chem. 257 (2000) 31219.
[3] T. Umemura, H. Hirohara, in: J.R.Whitaker, P.E. Sonnet (Eds.), Biocatalysis in Agricultural Biotechnology, American Chemical Society, Washington, DC, 1989 (Chapter 26).
[4] R.L. Kazlauskas, A.N.E. Weissfloch, A.T. Rappaport, L.A. Cuccia, J. Org. Chem. 56 (1991) 2656.
[5] N.N. Gandhi, N.S. Patil, S.B. Sawant, J.B. Joshi, P.P. Wangikar, D. Mukesh, Catal. Rev. Sci. Eng. 46 (2000) 439.
[6] J.K. Browne, M.A. McKervey, M. Pitarch, J.A. Russel, J.S. Millership, Tet. Lett. 39 (1998) 1787.
[7] B. Botta, M.C. Di Giovanni, O. Delle Monache, M.C. De Rosa, E. Gacs-Baitz, M. Botta, F. Corelli, A. Tafi, A. Santini, E. Benedetti, C. Pedone, D. Misiti, J. Org. Chem. 53 (1994) 1532.
[8] F. Mohamadi, N.G.J. Richards, W.C. Guida, C. Liskamp, G. Caufield, G. Chang, T. Hendrickson, W.C. Still, J. Comput. Chem. 11 (1990) 440.
[9] U. Derewenda, A.M. Brzozowski, A.M. Lawson, Z.S. Derewenda, Biochemistry 31 (1992) 1532.
[10] M. Botta, E. Cernia, F. Corelli, F. Manetti, S. Soro, Biochim. Biophys. Acta 1337 (1997) 302.
[11] A.E.M. Janssen, P.J. Hailing, J. Am. Chem. Soc. 116 (1994) 9827.
[12] R. Affieck, C.A. Haynes, D.S. Clark, Proc. Nat. Acad. Sci. 116 (1992) 5167.
[13] A. Tafi, A. van Almsick, F. Corelli, M. Crusco, K.B. Laumen, M.P. Schneider, J. Org. Chem. 65 (2000) 3659.
[14] R.J. Kazlauskas, Curr. Opin. Chem. Biol. 4 (2000) 81.
[15] J.J. De Voss, O. Sibbesen, Z. Zhang, P.R. Ortiz de Montellano, J. Am. Chem. Soc. 119 (1997) 5489.
[16] M. Cylger, P. Grochuiski, R.J. Kazlauskas, J.D. Schrag, F. Bouthillier, B. Rubin, A.N. Serreqi, A.K. Gupta, J. Am. Chem. Soc. 116 (1994) 3180.
[17] F. Manetti, F. Corelli, N. Mongelli, A. Lombardi Borgia, M. Botta, J. Computer-Aided Mol. Des. 14 (2000) 355.